

Controlling ultracold atoms in multi-band optical lattices for simulation of Kondo physics

L.-M. Duan

Department of Physics and FOCUS center, University of Michigan, Ann Arbor, MI 48109

We show that ultracold atoms can be controlled in multi-band optical lattices through spatially periodic Raman pulses for investigation of a class of strongly correlated physics related to the Kondo problem. The underlying dynamics of this system is described by a spin-dependent fermionic or bosonic Kondo-Hubbard lattice model even if we have only spin-independent atomic collision interaction. We solve the bosonic Kondo-Hubbard lattice model through a mean-field approximation, and the result shows a clear phase transition from the ferromagnetic superfluid to the Kondo-singlet insulator at the integer filling.

PACS numbers: 03.75.Fi, 03.67.-a, 42.50.-p, 73.43.-f

Ultracold atoms in optical lattices have recently received a lot of attention from both theoretical and experimental sides [1–14]. This system provides a platform to study strongly correlated many-body physics in a highly controllable environment. The underlying interaction Hamiltonians can be engineered by diverse methods. This engineered system, on the one hand, can be used to simulate various other strongly correlated systems which are less controllable for achieving a better understanding of the involved physics, and on the other hand, can implement new model Hamiltonians which may show novel strongly correlated phenomena [8].

In this paper we describe a technique to control ultracold atoms in multi-band optical lattices for investigation of a class of strongly correlated physics related to the famous Kondo problem. The Kondo problem arose from study of the magnetic impurities in metals [15]. Most of the latest investigations in this direction concentrate on the study of the lattice version of the Kondo model which is believed to be important for understanding the behavior of heavy-fermion and high- T_c superconducting compounds [15,16]. Here, we show that the Kondo interaction naturally arises in the ultracold system. By applying spatially periodic Raman pulses, we can control the atomic population in each band of the optical lattice. We show that with an integer filling of the lowest band, the underlying dynamics of this system is described by the Kondo-Hubbard lattice model, which is a hybridization of the Hubbard and the Kondo lattice models. The interaction parameters in this model can be well tuned by controlling the depth of the optical lattice, and this controlled realization could shed new light on understanding of this complicated theoretical model. We can realize both bosonic and fermionic versions of the Kondo-Hubbard lattice model, and in the case of bosonic atoms, we solve the model through a mean-field approximation, and the result shows a clear phase transition from the Ferromagnetic superfluid to the Kondo-

singlet insulator, arising from competition between the condensate-mediated magnetic interaction and the local Kondo interaction.

In condensed matter systems, the effective Kondo lattice model comes from perturbation of the Anderson lattice model in some parameter region [15,16]. A recent work has proposed an interesting scheme to realize the Anderson lattice model with fermionic atoms in a designed optical superlattice [12], which could lead to an effective Kondo model under precise control of some interaction parameters. In our approach, the Kondo interaction comes from a completely different origin. In a multi-band optical lattice, surprisingly, the Kondo interaction can be derived directly from the atomic collision interaction, even in the case that the latter is spin-independent. As here the Kondo interaction is a non-perturbative effect, it is much stronger compared with other approaches and should be ready for observation with the available experimental technology. In particular, we note that intriguing experiments have been reported on control of dilute (non-interacting) atoms in multi-band optical lattices [17–19], and extension of that ability should allow for demonstration of the model proposed here. We also note the recent interesting proposals on implementation of the impurity Kondo model with ultracold atoms in different contexts [10,11].

The ultracold atoms considered here can be either bosonic or fermionic. These atoms are first loaded into the lowest band of a 3-dimensional optical lattice, which is formed by standing-wave laser beams [1]. The optical potential barrier is high enough so that the atoms in the lowest band experience no tunneling. We then transfer part of the atomic population to an upper band, and the remaining atomic population in the lowest band is controlled to be one per each lattice site. We will show later how to achieve this through optical control. The atoms in the upper band undergo tunneling. If we neglect the atomic collision interaction, the non-interacting Hamiltonian for this system takes the following diagonal form

$$H_f = \epsilon_l \sum_{\mathbf{k}, \sigma} b_{\mathbf{k}\sigma}^\dagger b_{\mathbf{k}\sigma} + \sum_{\mathbf{k}, \sigma} \epsilon_{uk} a_{\mathbf{k}\sigma}^\dagger a_{\mathbf{k}\sigma}, \quad (1)$$

where the bosonic or fermionic annihilation operators $b_{\mathbf{k}\sigma}$ and $a_{\mathbf{k}\sigma}$ correspond respectively to the atoms in the lowest or the upper bands, with the Bloch wave vector \mathbf{k} and the spin component σ . For simplicity, we consider the atoms with two relevant Zeeman sublevels, for which the effective spin component σ takes two values \uparrow or \downarrow . For example, the atoms could be the fermionic Li^6 ($F = 1/2$)

or the bosonic Rb⁸⁷ or Na²³ ($F = 1$) while the Zeeman sublevel $|M_F = 0\rangle$ is made de-coupled by raising its energy [20]. The lowest band energy ϵ_l is \mathbf{k} -independent as the tunneling for this band is negligible.

The atomic collision interaction in free space is described by the Hamiltonian

$$H_I = \lambda_s \sum_{\sigma, \sigma'} \int d^3\mathbf{r} \Psi_{\sigma}^{\dagger}(\mathbf{r}) \Psi_{\sigma'}^{\dagger}(\mathbf{r}) \Psi_{\sigma'}(\mathbf{r}) \Psi_{\sigma}(\mathbf{r}), \quad (2)$$

where λ_s is the interaction parameter and $\Psi_{\sigma}(\mathbf{r})$ is the field operator with the spin σ . For simplicity we have assumed that the collision interaction is spin-independent as the spin-dependent collision terms are typically smaller by orders of magnitudes [21]. In a two-band optical lattice considered here, we should expand the field operator as $\Psi_{\sigma}(\mathbf{r}) = \sum_i [b_{i\sigma} w_l(\mathbf{r} - \mathbf{r}_i) + a_{i\sigma} w_u(\mathbf{r} - \mathbf{r}_i)]$, where $w_l(\mathbf{r} - \mathbf{r}_i)$ ($w_u(\mathbf{r} - \mathbf{r}_i)$) are the Wannier functions centered on the site i for the lowest (upper) band, and $\beta_{i\sigma} = \sum_{\mathbf{k}} \beta_{\mathbf{k}\sigma} e^{-i\mathbf{k} \cdot \mathbf{r}_i} / \sqrt{N}$ ($\beta = a, b$) with N being the number of lattice sites. Substituting this expansion into H_I , we can derive the expression for the total Hamiltonian $H = H_f + H_I$. Under a number of approximations specified below, the Hamiltonian H in the rotating frame has the form

$$H = \sum_{\mathbf{k}, \sigma} \bar{\epsilon}_{u\mathbf{k}} a_{\mathbf{k}\sigma}^{\dagger} a_{\mathbf{k}\sigma} + u_h \sum_i n_i (n_i - 1) + (-1)^{\nu} u_c \sum_i \mathbf{s}_{i\beta} \cdot \mathbf{s}_{i\alpha}, \quad (3)$$

where $\nu = 0$ for bosons and $\nu = 1$ for fermions. In Eq. (3), the number operator $n_i = \sum_{\sigma} a_{i\sigma}^{\dagger} a_{i\sigma}$, the three components of the spin operator $\mathbf{s}_{i\beta}$ ($\beta = a, b$) are defined by $\mathbf{s}_{i\beta}^z = (\beta_{i\uparrow}^{\dagger} \beta_{i\uparrow} - \beta_{i\downarrow}^{\dagger} \beta_{i\downarrow})/2$, $\sigma_i^x = (\beta_{i\uparrow}^{\dagger} \beta_{i\downarrow} + \beta_{i\downarrow}^{\dagger} \beta_{i\uparrow})/2$, and $\sigma_i^y = -i(\beta_{i\uparrow}^{\dagger} \beta_{i\downarrow} - \beta_{i\downarrow}^{\dagger} \beta_{i\uparrow})/2$, and the coefficients $u_h = \lambda_s \int |w_u(\mathbf{r} - \mathbf{r}_i)|^4 d^3\mathbf{r}$, $u_c = 4\lambda_s \int |w_l(\mathbf{r} - \mathbf{r}_i)|^2 |w_u(\mathbf{r} - \mathbf{r}_i)|^2 d^3\mathbf{r}$ (assuming that the Wannier functions are normalized). The shifted energy $\bar{\epsilon}_{u\mathbf{k}} = \epsilon_{u\mathbf{k}} - \bar{\epsilon}_u$, where $\bar{\epsilon}_u$ is the average energy in the upper band. If the band energy $\bar{\epsilon}_{u\mathbf{k}}$ takes the form of $\bar{\epsilon}_{u\mathbf{k}} = -2t(\cos k_x a_c + \cos k_y a_c + \cos k_z a_c)$ (a_c is the lattice constant for the cubic lattice) under the tight-binding approximation, the first term of the Hamiltonian (3) has the more familiar form $-t \sum_{\langle i, j \rangle, \sigma} (a_{i\sigma}^{\dagger} a_{j\sigma} + H.c.)$, where t characterizes the nearest-neighbor tunneling rate and $\langle i, j \rangle$ stands for all the neighboring sites. In deriving Eq. (3), we have also made the following approximations or assumptions: (i) the band gap $\Delta = \bar{\epsilon}_u - \epsilon_l$ is assumed to be much larger than the coefficients t, u_h, u_c which justifies the rotating-wave approximation; (ii) we keep only the on-site collision interaction terms for both the lowest and the upper bands; (iii) we have assumed one atom per each site for the lowest band; (iv) the Hamiltonian has been transferred to the rotating frame by dropping the free-energy terms

$\epsilon_l \sum_{i\sigma} b_{i\sigma}^{\dagger} b_{i\sigma} + [\bar{\epsilon}_u + (2 + (-1)^{\nu}) u_c/4] \sum_{i\sigma} a_{i\sigma}^{\dagger} a_{i\sigma}$. All these approximations or assumptions will be justified from our later numerical calculation of the lattice structure.

The Hamiltonian (3) represents a hybridization of the Kondo lattice model and the Hubbard model. For bosonic atoms, the Kondo interaction (the last term of Eq. (3)) is antiferromagnetic with the repulsive interaction ($\lambda_s > 0$), and ferromagnetic with the attractive interaction ($\lambda_s < 0$), while the reverse is the case for fermionic atoms due to the different commutation relation. Typically, the Kondo interaction is comparable in magnitudes with the Hubbard interaction. However, the ratio u_h/u_c can be tuned by controlling the depth of the optical lattice and/or by going to different upper bands. With change of the optical lattice depth, the tunneling energy t can also be adjusted sensitively (see Fig. 1D). So, a variety of interesting physics could be associated with the Hamiltonian (3) as we change the interaction types or tune the ratios of different kinds of interaction strengths. Such an extent of the controllability, if experimentally realized, would lead to significant breakthrough in investigation of the Kondo physics.

Before studying the ground-state properties of the Kondo-Hubbard lattice model (3), first we would like to show how to control the atomic population in each band as we have assumed, and to justify the approximations made in our derivation of the Hamiltonian (3). For this purpose, we need to know the exact band structure of the optical lattice. Though the lowest band can be calculated easily through the harmonic approximation to the potential wells, this approximation is in general not valid for upper bands, and we find it more convenient to numerically solve the exact band structure.

The trapping potential from standing wave lasers has the form $V(\mathbf{r})/E_R = V_0 (\sin^2 k_0 x + \sin^2 k_0 y + \sin^2 k_0 z)$, where k_0 is the laser wave vector and we take the atomic recoil energy $E_R = \hbar^2 k_0^2 / 2m$ (m is the mass of the atom) as the energy unit so that the potential barrier V_0 is dimensionless. The band structure is determined by solving the one-particle Schrodinger equation $-\nabla^2 \Phi / k_0^2 + [V(\mathbf{r})/E_R] \Phi = E \Phi$, where E is the band energy in the unit of E_R . This equation can be reduced to the 1-dimensional Schrodinger equation by separating variables $\Phi(\mathbf{r}) = \Phi_x(x) \Phi_y(y) \Phi_z(z)$, and we can expand the wave function in each direction as superposition of the plane waves, for instance, $\Phi_x(x) = \sum_n a_{n, k_x} e^{i(2nk_0 + k_x)x}$, where k_x is the Bloch wave vector in x direction. We take the superposition coefficients a_{n, k_x} as the variational parameters to numerically minimize the band energy $E = E_x + E_y + E_z$. In this way, we find the exact band structure. With a typical potential barrier $V_0 = 30$, the band energy E_x is shown in Fig. 1A for the lowest five bands. From the solution of the variational parameters a_{n, k_x} , we can also construct the Bloch wave function $u_{k_x}(x) = \sum_n a_{n, k_x} e^{i2nk_0 x}$ and the Wannier function $w_x(x - x_i) = \sum_{k_x} u_{k_x} e^{ik_x(x - x_i)} / \sqrt{N}$

in x direction (the same expression holds in other directions). The Wannier function $w_x(x)$ is shown in Fig. 1E for the lowest three bands.

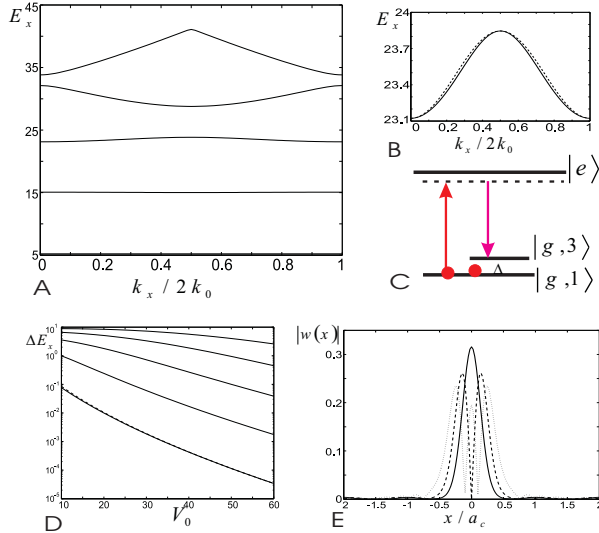


FIG. 1. (A) The band structure of the optical lattice with the potential barrier $V_0 = 30$. The energy E_x (in the unit of E_R) of the lowest five bands is shown as a function of the normalized Bloch wave vector $k_x/2k_0$. (B) The enlarged structure of the 3rd band (the solid curve) compared with the fit from the cosine function (the dashed curve). (C) The illustration of the energy-selective Raman pulses which transfer one atom to the third band within the same internal state $|g\rangle$. (D) The widths ΔE_x (proportional to the tunneling rate) of the lowest five bands shown as functions of the potential barrier V_0 . (E) The magnitudes of the Wannier functions for the lowest (the solid curve), the second (the dashed curve), and the third (the dotted curve) bands.

To manipulate the atomic population in each band, we propose to use spatially periodic Raman pulses to transfer atoms from the lowest band to a specified upper band as shown in Fig. 1C. Note that a spatially homogeneous Raman pulse can not change the atoms' external state as the Wannier functions for different bands are orthogonal to each other. We can simply apply standing wave Raman pulses with the same period as the optical lattice. For instance, two Raman beams of the form of $\cos k_0 x$ (the Raman Rabi frequency $\Omega_R \propto \cos^2 k_0 x$) with a frequency difference matching the band gap $\Delta = E_{x3} - E_{x1}$ will transfer the atoms from the lowest band to the third band in the x direction. Note that the atoms are still in the lowest band for the y, z directions, so they only tunnel along the x direction and the resulting model is essentially 1-dimensional although we have a 3-dimensional lattice. We can get higher-dimensional Kondo-Hubbard lattice models by exciting the atoms to upper bands in several directions. For instance, two Raman beams of the forms of $\cos k_0 x, \cos k_0 y$ respectively ($\Omega_R \propto \cos k_0 x \cos k_0 y$) will transfer the atoms to upper bands in both x and y directions, and intensity superpositions of the Raman

pulses with Rabi frequencies $\Omega_{R1} \propto \cos k_0 (x + y) \cos k_0 z$, $\Omega_{R2} \propto \cos k_0 (x - y) \cos k_0 z$ respectively will transfer the atoms to upper bands in all the three dimensions (Note that $\Omega_{R1} + \Omega_{R2} \propto \cos k_0 x \cos k_0 y \cos k_0 z$).

We make use of the collision shift of the band energy to control the atom number in the lowest band to be one per each lattice site. Assume that we start with a Mott insulator state with all the atoms in the lowest band, and the average filling number of the lattice is between 1 and 2. In this case, some lattice sites have two atoms while others have one. We apply the Raman pulses to transfer one atom to the upper band only for the lattice sites with two atoms (see Fig. 1C). This is possible because the collision energy shift depends on which bands the atoms are. One can choose a right frequency difference for the Raman beams so that only the desired two-photon transition is resonant. All the other transitions are detuned by the difference in the collision energy shifts, which is typically about a few kHz [1]. So the Raman beams with the two-photon Rabi frequency significantly smaller than kHz will achieve the desired distribution of the atomic population.

All the approximations made in the derivation of the Hamiltonian (3) are well justified by our calculation of the lattice structure: firstly, from Fig. 1A, the band gap $\Delta \approx 18E_R$ if we choose the third band as the upper band, which is much larger than the relevant energies t, u_h, u_c (typically around E_R). Secondly, as shown in Fig. 1E, the Wannier functions are well localized even for the upper bands. For the third band with $V_0 = 30$, the nearest neighbor collision rate is only 0.2% of the on-site collision rate, which can be safely neglected. The nearest neighbor tunneling has the dominant contribution to the band width as shown in Fig. 1B ($\bar{\epsilon}_{uk}$ is approximated by the cosine form). Finally, the tunneling rate (the width) for each band can be sensitively detuned through control of the potential barrier V_0 as shown in Fig. 1D.

The Kondo-Hubbard lattice model shows interesting quantum phase transition arising from competition of different types of interactions. Here, as an example, we investigate the bosonic Kondo-Hubbard lattice model with $u_c > 0$ as it is easier to be realized experimentally and not encountered yet in the literature to the best of our knowledge. We solve the model through a mean-field approximation by assuming that the ground-state of the Hamiltonian (3) is not entangled for different lattice sites. This approximation corresponds to a generalization of the popular Guzwiller ansatz for the bosonic case [22,3], which usually gives good results in particular in the strong interaction region.

With this mean-field approximation, the ground state energy of the Hamiltonian (3) per each site is given by

$$E_i = -\Delta E_u \sum_{\sigma} |\langle a_{i\sigma} \rangle|^2 + u_h \langle n_i^2 - n_i \rangle + u_c \langle \mathbf{s}_{ib} \cdot \mathbf{s}_{ia} \rangle,$$

where ΔE_u is the half band width, which is $z_c |t|$ (z_c is the coordination number) if only the nearest neighbor

tunneling is taken into account. The energy E_i can be numerically minimized by assuming a variational form for the ground state $|\Psi_i\rangle = \sum_{mn\sigma} c_{mn\sigma} |m_\uparrow\rangle_{a_\uparrow} |m_\downarrow\rangle_{a_\downarrow} |\sigma\rangle_b$, where $\sigma = \uparrow, \downarrow$, $|m_\uparrow\rangle_{a_\uparrow}, |m_\downarrow\rangle_{a_\downarrow}$ are number states of the modes a_\uparrow, a_\downarrow , and $c_{mn\sigma}$ are variational parameters. The minimization is subject to the constraints $\langle\Psi_i|\Psi_i\rangle = 1$ and $\langle\Psi_i|n_i|\Psi_i\rangle = \bar{n}$, where \bar{n} is the average filling number of the upper band. The properties of this system can be determined from the variational ground state. The particularly interesting quantities include the superfluid magnitude defined as $S_{\text{sup}} = \sum_{\sigma} |\langle a_{i\sigma} \rangle| / \sqrt{a_{i\sigma}^\dagger a_{i\sigma}}$, and the magnetizations of the lowest and the upper bands given respectively by $M_b = |\langle \mathbf{s}_{ib} \rangle|$, $M_a = |\langle \mathbf{s}_{ia} \rangle|$.

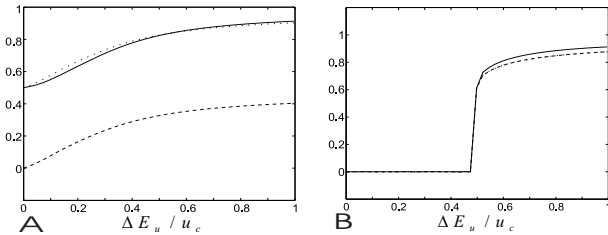


FIG. 2. (A) The superfluid magnitude (the solid curve), the lowest band magnetization (the dotted curve), and the upper band magnetization (the dashed curve) shown as functions of the energy ratio $\Delta E_u / u_c$ with the upper-band mean filling number $\bar{n} = 1/2$. For this calculation, we have taken $\Delta u_h / u_c = 1.52 / (4 \times 0.84) = 0.45$, corresponding to the real value with the potential barrier $V_0 = 30$. (B) The same as Fig. 2A except that the mean filling number $\bar{n} = 1$.

Figure 2 shows the calculation results for the quantities defined above with the filling number $\bar{n} = 1/2$ and $\bar{n} = 1$, respectively. At the integer filling, clearly there is a phase transition at the point $\Delta E_u / u_c \sim 0.5$ (see Fig. 2B). If the tunneling rate (characterized by ΔE_u) is below this threshold value, each site is occupied by two atoms at two different bands, forming a local Kondo signet $(|\uparrow\downarrow\rangle_{ba} - |\downarrow\uparrow\rangle_{ba}) / \sqrt{2}$ to minimize the energy of the anti-ferromagnetic coupling $\mathbf{s}_{ib} \cdot \mathbf{s}_{ia}$. So there are no superfluid magnitude and no magnetizations in both bands. As soon as the tunneling rate across this threshold, both the superfluid magnitude and the magnetizations quickly go up. In this case, the atoms in the upper band actually form a ferromagnetic condensate to minimize the kinetic (tunneling) energy, while the atoms in the lowest band are magnetized in the reverse direction to minimize the energy $\mathbf{s}_{ib} \cdot \mathbf{s}_{ia}$. There are long-range correlations both in magnetization and in the superfluid phase. However, at the non-integer filling, all the quantities change continuously (See Fig. 2B). As soon as the tunneling rate is nonzero, the holes in the upper band can move in the lattice and there is no energy penalty for that. To maximize the tunneling effect (the kinetic energy), it is better that all the unpaired atoms in the lowest band are polarized along the same direction. So the lowest band magnetization and the superfluid magnitude starts from

a significant non-zero value, while the upper band magnetization needs to gradually increase from zero as most of the atoms in this band are still paired in the Kondo signets.

At the end of the paper, we would like to briefly discuss how to observe the above phenomena in experiments. The superfluid magnitude can be measured through observing the atomic interference as in the experiment [1]. The atoms in different bands can be separated through the Landau-Zener tunneling by accelerating the lattice with an appropriate speed [17,18,13]. To detect magnetization in each band, the atomic spin states can be measured through a Stern-Gerlach experiment or through spin-dependent light absorption. Note that the energy scale in our model is characterized by t, u_h, u_c , which are typically about a few kHz. The temperature achieved already in the experiment [1] should allow demonstration of this model.

This work was supported by the Michigan start-up fund and by the FOCUS center.

-
- [1] M. Greiner *et al.*, Nature 415, 39 (2002).
 - [2] C. Orzel *et al.*, Science 291, 2386 (2001).
 - [3] D. Jaksch, *et al.*, Phys. Rev. Lett. **81**, 3108 (1998).
 - [4] E. Demler, F. Zhou, Phys. Rev. Lett. **88**, 163001 (2002).
 - [5] W. Hofstadter *et al.*, Phys. Rev. Lett. **89**, 220407.
 - [6] A. Recati, P.O. Fedichev, W. Zwerger, and P. Zoller, Phys. Rev. Lett. **90**, 020401 (2003).
 - [7] B. Paredes and J. I. Cirac, Phys. Rev. Lett. **90**, 150402 (2003).
 - [8] L.-M. Duan, E. Demler, M. D. Lukin, Phys. Rev. Lett. **91**, 090402 (2003).
 - [9] B. Damski *et al.*, Phys. Rev. Lett. **91**, 080403 (2003).
 - [10] A. Recati *et al.*, cond-mat/0212413.
 - [11] G.M. Falco, R.A. Duine, H. Stoof, cond-mat/0304489.
 - [12] B. Paredes, C. Tejedor, J. I. Cirac, cond-mat/0306497.
 - [13] B. Wu, Q. Niu, cond-mat/0306411.
 - [14] R. Roth, K. Burnett, cond-mat/0310114.
 - [15] A.C. Hewson *The Kondo problem to Heavy Fermions*, Cambridge University Press, Cambridge, UK (1997).
 - [16] H. Tsunetsugu, M. Sigrist, K. Ueda, Rev. Mod. Phys. **69**, 809 (1997).
 - [17] S. R. Wilkinson *et al.*, Phys. Rev. Lett. **76**, 4512 (1996).
 - [18] C. F. Bharucha *et al.*, Phys. Rev. A **55**, R857 (1997).
 - [19] B. K. Teo, J. R. Guest, and G. Raithel, Phys. Rev. Lett. **88**, 173001 (2002).
 - [20] A. Sorensen *et al.*, Nature 409, 63 (2001).
 - [21] D. M. Stamper-Kurn and W. Ketterle, cond-mat/0005001.
 - [22] W. Krauth, M. Caffarel, J.-P. Bouchaud, Phys. Rev. B **45**, 3137 (1992).